SCG10 is a JNK target in the axonal degeneration pathway

Jung Eun Shin[a,1], Bradley R. Miller[a,1,2], Elisabetta Babetto[a], Yongcheol Cho[b], Yo Sasaki[c], Shehzad Qayum[a], Emilie V. Russler[a], Valeria Cavalli[b,d], Jeffrey Milbrandt[c,d], and Aaron DiAntonio[a,d,3]

Departments of [a]Developmental Biology, [b]Anatomy and Neurobiology, and [c]Genetics, and [d]Hope Center for Neurological Disorders, Washington University School of Medicine, St. Louis, MO 63110

Edited by Don W. Cleveland, University of California at San Diego, La Jolla, CA, and approved October 22, 2012 (received for review September 19, 2012)

Axons actively self-destruct following genetic, mechanical, metabolic, and toxic insults, but the mechanism of axonal degeneration is poorly understood. The JNK pathway promotes axonal degeneration shortly after axonal injury, hours before irreversible axon fragmentation ensues. Inhibition of JNK activity during this period delays axonal degeneration, but critical JNK substrates that facilitate axon degeneration are unknown. Here we show that superior cervical ganglion 10 (SCG10), an axonal JNK substrate, is lost rapidly from mouse dorsal root ganglion axons following axotomy. SCG10 loss precedes axon fragmentation and occurs selectively in the axon segments distal to transection that are destined to degenerate. Rapid SCG10 loss after injury requires JNK activity. The JNK phosphorylation sites on SCG10 are required for its rapid degradation, suggesting that direct JNK phosphorylation targets SCG10 for degradation. We present a mechanism for the selective loss of SCG10 distal to the injury site. In healthy axons, SCG10 undergoes rapid JNK-dependent degradation and is replenished by fast axonal transport. Injury blocks axonal transport and the delivery of SCG10, leading to the selective loss of the labile SCG10 distal to the injury site. SCG10 loss is functionally important: Knocking down SCG10 accelerates axon fragmentation, whereas experimentally maintaining SCG10 after injury promotes mitochondrial movement and delays axonal degeneration. Taken together, these data support the model that SCG10 is an axonal-maintenance factor whose loss is permissive for execution of the injury-induced axonal degeneration program.

Axon loss is a devastating consequence of a wide range of neurological diseases. A hallmark of hereditary neuropathies, glaucoma, and diabetic neuropathy, axon loss also is found early in the progression of debilitating neurodegenerative diseases such as Alzheimer's and Parkinson disease (1, 2). Although the great length of many axons is essential to their function, it also makes them vulnerable to mechanical trauma and to neurotoxins such as chemotherapeutics that interfere with axonal transport (3). Current therapies for axonal degeneration target either the systemic diseases that lead to axon loss or the pain that results from axon dysfunction (4). Therapies targeting the axon breakdown process itself are notably absent. Elucidating the mechanism of axonal degeneration may help to develop such therapies.

Axonal degeneration is an actively regulated process that is blocked by the overexpression of the Wallerian degeneration slow (Wld^S) fusion protein or its enzymatically active component NMNAT (5–10). Regulated protein degradation promotes the degeneration of injured axons (11), potentially via the degradation of labile axonal-maintenance factors. Rapid postinjury loss of axonal-maintenance factors is a likely mechanism for promoting axon degeneration. NMNAT2 is the first identified axonal-maintenance factor that is degraded soon after injury. Its loss triggers axonal degeneration, and forced expression of NMNAT2 delays axonal degeneration (12). It is not known whether other axonal-maintenance factors are lost rapidly after injury or whether signaling pathways that control the timing of axonal degeneration regulate such maintenance factors.

JNKs are MAPKs that are central to the axonal-injury response. Depending on the context, axonal injury can result in neuronal apoptosis, axonal regeneration, or axonal degeneration, and JNK is required for each of these varied responses (13–21). The JNK pathway is required for axonal degeneration shortly after injury and many hours before axon fragmentation: JNK inhibition at the time of injury effectively delays degeneration, but inhibition starting during the subsequent active fragmentation phase has no effect (16), thus suggesting that JNK activity early in the postinjury period commits injured axons to degenerate. However, the mechanism by which JNK promotes the axonal commitment is unknown. Blocking this commitment step before irreversible axon fragmentation occurs is an attractive therapeutic approach. Although JNK itself is a promising target, indiscriminate JNK inhibition also might produce undesirable effects, given its diverse roles in the nervous system. An alternative is to identify the relevant JNK substrates for axonal degeneration. Because axon fragmentation is delayed when a JNK inhibitor is added to severed distal axons, the relevant substrate or substrates must be axonal proteins (16).

Superior cervical ganglion 10 (SCG10) is a microtubule-binding protein in axons that is a substrate of JNK (22). Through its direct binding of tubulin heterodimers, SCG10 modulates axonal microtubule dynamic instability (23). Phosphorylation of SCG10 by JNK on serines 62 and 73 dramatically decreases its affinity for tubulin and thereby alters the balance between microtubule assembly and disassembly (24). Here we demonstrate that SCG10 is a labile axonal protein rapidly degraded in healthy axons in a JNK-dependent manner. Axonal SCG10 normally is replenished by fast axonal transport. However, upon axonal injury, axonal transport is interrupted, leading to the loss of SCG10 in the distal axon. The abundance of axonal SCG10 is functionally important for the preservation of injured axons: Experimental depletion of SCG10 results in accelerated degeneration of injured axons, and enforced maintenance of SCG10 levels in axons following injury is sufficient to delay degeneration. These data demonstrate that SCG10 is an axonal-maintenance factor whose loss is permissive for injury-induced axonal degeneration.

Author contributions: J.E.S., B.R.M., V.C., J.M., and A.D. designed research; J.E.S., B.R.M., E.B., Y.C., Y.S., S.Q., and E.V.R. performed research; J.E.S., B.R.M., E.B., Y.C., S.Q., and E.V.R. analyzed data; and J.E.S., B.R.M., J.M., and A.D. wrote the paper.

Conflict of interest statement: A.D., J.E.S., and Washington University may receive income based on a license by the University to Novus Biologicals.

This article is a PNAS Direct Submission.

[1]J.E.S. and B.R.M. contributed equally to this work.

[2]Present address: Department of Psychiatry, Columbia University, New York, NY 10032; and The New York State Psychiatric Institute, New York, NY 10032.

[3]To whom correspondence should be addressed. E-mail: diantonio@wustl.edu.

See Author Summary on page 21199 (volume 109, number 52).

This article contains supporting information online at www.pnas.org/lookup/suppl/doi:10.1073/pnas.1216204109/-/DCSupplemental.

Results

SCG10 Is Lost Rapidly from Injured Distal Axons. SCG10 is an axonal protein whose regulation of microtubule dynamics is altered by JNK phosphorylation (22, 24) and therefore is a potentially important downstream effector of JNK-mediated axonal fragmentation following axonal injury. In previous work using a dorsal root ganglion (DRG) in vitro model of axonal injury, we showed that JNK activity is required during the first 3 h after axotomy for the subsequent rapid initiation of axonal degeneration (16). We used this system to test the hypothesis that injury leads to the JNK-dependent phosphorylation of SCG10. DRG neurons were cultured for 9 d in vitro (DIV) before axon transection under conditions in which axon fragmentation begins ~6 h after injury. To assess the effects of axon injury on SCG10, we prepared protein lysates 3 h after axotomy (i.e., before axon fragmentation occurred) from distal axon segments and from intact control axons. Western blot analysis detected multiple SCG10 species migrating at ~20 kDa in intact axons, as previously reported (22, 24). However, instead of the expected increase in the slower migrating, phosphorylated SCG10 species in distal segments of injured axons, we found that SCG10 levels were decreased dramatically in these severed axon segments. Indeed, at this early time point 3 h postinjury, SCG10 levels were decreased more than 80% [81 ± 4% decrease (mean ± SEM); $n = 4$; $P < 0.001$] (Fig. 1*A*). The rapidity of SCG10 loss, before any evidence of axonal fragmentation, suggests that it is an early marker of axonal injury rather than a consequence of axonal breakdown. To test this hypothesis, we used lentivirus to express a cytoplasmic NMNAT1 mutant (cytNmnat1) that robustly prevents axon degeneration (25). We found that SCG10 is lost rapidly from distal axons after injury even though cytNmnat1 overexpression prevents axonal degeneration [83 ± 2% decrease in injured control axons; 82 ± 2% decrease in injured cytNmnat1 axons (mean ± SEM); $n = 6$; $P > 0.8$] (Fig. 1*B*). Thus, SCG10 degradation is not a consequence of axonal degeneration; instead, it is an early event in the response to axonal damage.

Next, we set out to determine if SCG10 is lost rapidly after axonal injury in vivo. We transected the sciatic nerve in adult mice and 3 h later harvested the nerve segments distal to the site of injury. Although axons do not degenerate until ~48 h after transection in vivo (26), we chose this very early postinjury time point to assess again whether SCG10 loss is an early event in the process rather than a consequence of axon fragmentation. Western blot analysis comparing SCG10 levels in intact nerve vs. distal segments showed a significant decrease in SCG10 levels within 3 h after injury [71 ± 7% decrease (mean ± SEM); $n = 5$; $P < 0.001$] (Fig. 1*C*). These data show that SCG10 levels decline rapidly in injured distal axon segments both in vitro and in vivo.

Although distal and proximal axon segments encounter the identical initial trauma after transection, segments distal to the injury site degenerate, whereas proximal axons survive and often regenerate. Because SCG10 is degraded in distal injured axons long before axonal fragmentation both in vitro and in vivo, SCG10 loss is a potential early indicator of whether an injured axon will degenerate. To determine if SCG10 is lost selectively in axons destined to degenerate, we compared SCG10 levels in DRG axons proximal and distal to the transection site 3 h after axotomy. We found that SCG10 is preserved in proximal axon segments (Fig. 1*D*). Indeed, there is an increase in SCG10 in severed proximal axon stumps relative to baseline levels [5.3 ± 0.5 fold increase (mean ± SEM); $n = 4$; $P < 0.001$] (Fig. 1*D*). Thus, SCG10 is lost selectively in distal axons, and SCG10 loss is an early marker of subsequent axon breakdown.

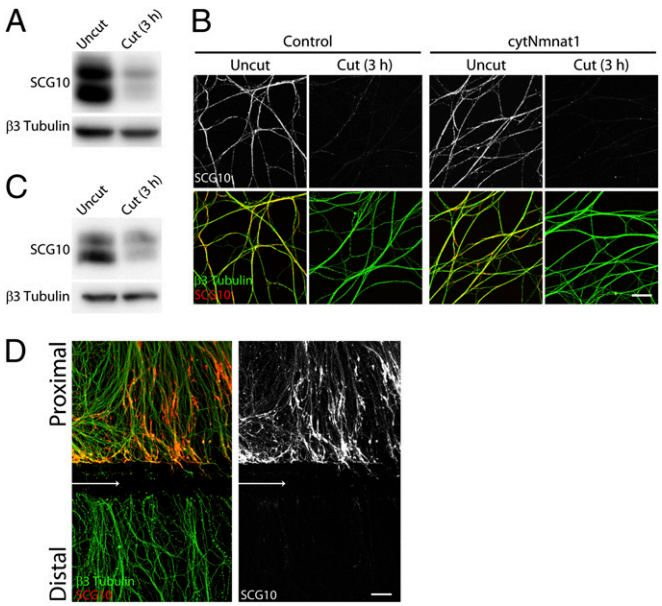

Fig. 1. SCG10 loss is an early marker of axonal injury. (*A*) Immunoblot analysis of endogenous SCG10 in cultured DRG axons with or without axotomy. The SCG10 level is decreased dramatically in the distal axons collected 3 h after axotomy compared with the level in the uncut control axons. Immunoblot against neuron-specific β3 tubulin confirms comparable amounts of protein loaded. (*B*) Axonal SCG10 is examined by immunostaining 3 h after axotomy in the DRG cultures infected with control or cytNmnat1-expressing lentivirus. The SCG10 level is decreased by axotomy to a similar extent in the distal axons of cytNmnat1-expressing neurons and in the control culture. β3 tubulin (green) labels microtubules in axons. (Scale bar, 50 μm.) (*C*) Three hours after sciatic nerve transection in adult mice, SCG10 levels were assayed by immunoblot in a control nerve and in the nerve segment distal to the axotomy. The SCG10 level is decreased significantly by axotomy. β3 tubulin is shown as a loading control. (*D*) SCG10 is lost selectively in the distal axons as shown by immunolabeling against SCG10 and β3 tubulin in the DRG cultures 3 h after axotomy. Arrows indicate the site of axotomy. SCG10 protein is accumulated in the proximal segment. (Scale bar, 50 μm.)

SCG10 Undergoes Rapid JNK-Dependent Turnover in Both Injured and Healthy Axons. SCG10 is a JNK substrate, and JNK promotes axon degeneration following axotomy. Therefore, we examined whether the SCG10 loss in severed axons is mediated by JNK activity. We tested if JNK activity during the early period after axonal injury is required for the loss of SCG10 by treating cultured DRG neurons at the time of axotomy with a JNK inhibitor, SP600125, that delays axonal degeneration (16, 21). We found that there is significantly less SCG10 loss in injured distal axons in neurons treated with SP600125 ($P < 0.01$ vs. axotomy and vehicle) (Fig. 2 *A* and *B*). These data demonstrate that JNK activity is required for the rapid loss of SCG10 following axonal injury.

After transection, SCG10 levels are dramatically different in the proximal and distal axon segments although the segments received the same initial mechanical injury. This difference may be caused by the selective activation of an SCG10 degradation signal in the distal axon segment. Alternatively, SCG10 normally might undergo rapid JNK-dependent turnover in axons, and therefore its levels would need to be maintained by continuous replenishment from the cell body via de novo synthesis and axonal transport. In this case, interruption of axonal transport by axotomy would prevent the resupply of SCG10, and axonal SCG10 levels would decrease after injury. If the same mechanism underlies normal SCG10 turnover and the injury-induced loss of SCG10 in distal axon segments, then healthy neurons treated with a JNK inhibitor should have increased SCG10 levels. We treated DRG neurons with the JNK inhibitor SP600125 and found that SCG10 levels were increased within 3 h ($P < 0.005$ vs. no axotomy and vehicle) (Fig. 2 *A* and *B*), indicating that JNK likely regulates SCG10 turnover in both healthy and injured axons. These data are consistent with a model wherein injury results in SCG10 loss in injured

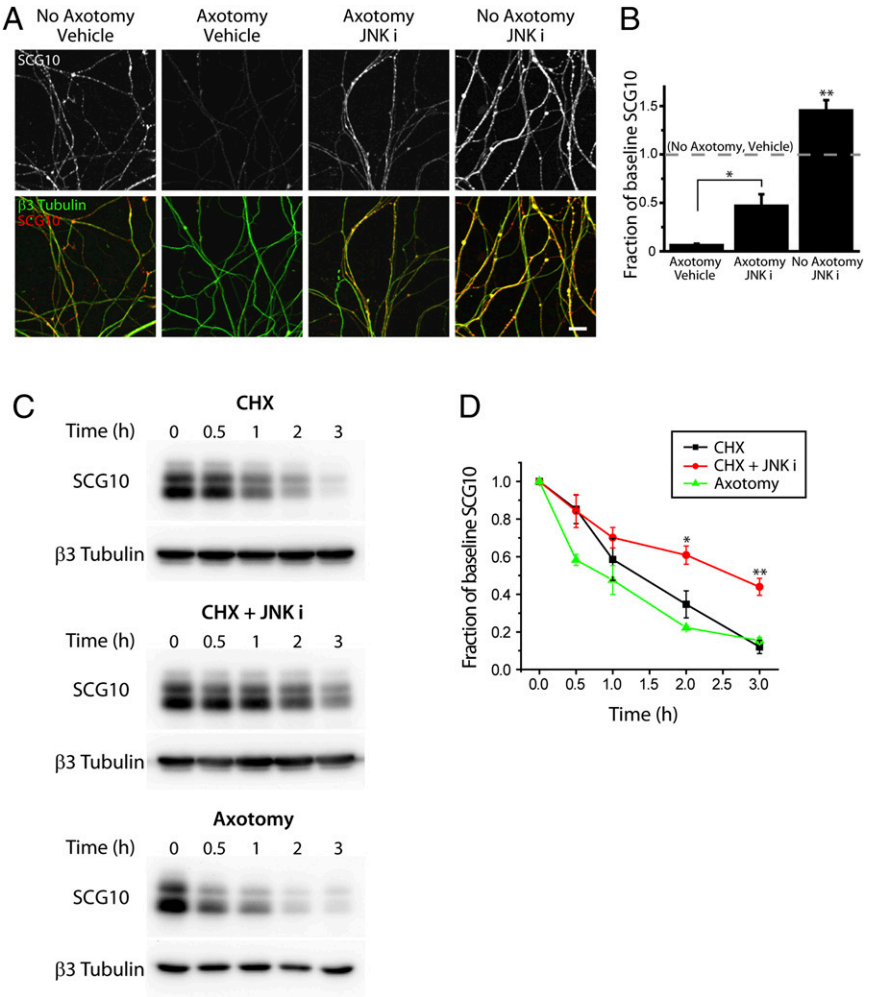

Fig. 2. The SCG10 level is regulated by JNK in healthy and injured axons. (*A*) Immunostaining for SCG10 is shown in the cultured DRG axons labeled with anti-β3 tubulin antibody. Neurons were axotomized for 3 h, and either vehicle (DMSO) or the JNK inhibitor SP600125 (JNK i; 15 μM) was applied at the time of axotomy. SCG10 loss after axotomy is significantly reduced by inhibiting JNK activity. JNK inhibition also causes a dramatic increase in SCG10 level in non-injured axons. (Scale bar, 30 μm.) (*B*) Results from *A* were quantified for the axonal SCG10 levels normalized to the baseline SCG10 level (dotted line, no axotomy and vehicle). Axonal SCG10 levels were obtained by calculating the average SCG10 immunofluorescence within the β3 tubulin-positive area. $n = 5$, axotomy and vehicle; $n = 5$, axotomy and JNKi; $n = 9$, no axotomy and JNKi. $^{*}P < 0.01$ for axotomy and JNK i vs. axotomy and vehicle (two-sample t test); $^{**}P < 0.005$ for no axotomy and JNK i vs. baseline level (one-sample t test). Error bars represent SEM. (*C*) Axonal SCG10 degradation was examined by immunoblot analyses on the axonal lysates. (*Top*) SCG10 degradation was examined by inhibiting protein synthesis in DRG neurons by CHX treatment for the indicated time. (*Middle*) SCG10 turnover is slowed by inhibition of JNK with 15 μM SP600125 (JNK i). (*Bottom*) SCG10 turnover after axotomy was assessed at the indicated times after axotomy. β3 tubulin is shown as a loading control. (*D*) Quantification of the results shown in *C*. SCG10 levels are plotted as the fraction of the SCG10 level at time 0. The rate of SCG10 turnover is comparable in CHX-treated axons and injured distal axons, although the beginning of SCG10 loss appears delayed in CHX-treated axons. JNK inhibition results in a significant decrease in the SCG10 turnover rate. $^{*}P < 0.05$, $^{**}P = 0.005$ vs. CHX by t test. $n = 3$ for each condition. Error bars represent SEM.

axons through lack of replenishment via normal protein synthesis and axonal transport.

As a direct test of the hypothesis that SCG10 is a labile axonal protein that continuously undergoes rapid degradation and replenishment, we examined its turnover in cultured DRG neurons. Western blot analysis was performed on axonal protein lysates from neurons grown in the protein synthesis inhibitor cycloheximide (CHX) for various lengths of time. We found that SCG10 levels decline rapidly (Fig. 2 *C* and *D*). The degree of SCG10 loss was similar to that found after axotomy: SCG10 levels were decreased to 12 ± 4% (mean ± SEM; $n = 3$) of baseline 3 h after CHX addition vs. 15 ± 2% (mean ± SEM; $n = 3$) 3 h after axotomy (Fig. 2*D*). The calculated half-life for SCG10 is somewhat longer following CHX treatment (1.5 h) than after axotomy (0.8 h) because of the time at which SCG10 loss begins. For instance, with axotomy there is significant SCG10 loss within 0.5 h ($P < 0.01$), whereas there is little decrease in SCG10 immediately after CHX treatment. This difference likely reflects the immediate block of SCG10 delivery resulting from axon severing as compared with the continued delivery of previously synthesized SCG10 molecules in the case of CHX treatment. Nevertheless, after this lag, the decline in SCG10 levels from 75 to 25% of baseline levels is similar under both conditions (1.7 h for CHX; 1.5 h for axotomy). This result is consistent with a model in which SCG10 loss after axotomy reflects basal SCG10 turnover.

To investigate the contribution of JNK activity to the basal degradation of SCG10, we treated DRG cultures with CHX in the presence or absence of SP600125. JNK inhibition significantly slowed the loss of SCG10, increasing the half-life from 1.5 to 2.5 h, thereby leading to a 3.7-fold increase in SCG10 levels after 3 h of CHX treatment ($P = 0.005$) (Fig. 2 *C* and *D*). This result directly demonstrates that JNK activity regulates the degradation of SCG10.

JNK Phosphorylation Targets SCG10 for Degradation. Our data indicate that SCG10 undergoes JNK-dependent degradation. Direct JNK phosphorylation of SCG10 may target it for degradation, or, alternatively, JNK may promote SCG10 degradation more indirectly. To address how JNK mediates SCG10 loss, we first assessed gel mobility of the SCG10 species that were preserved by either JNK inhibition or protease inhibition in injured axons. Phosphorylated SCG10 runs at a higher molecular weight than nonphosphorylated SCG10 (22, 24). Therefore, if JNK phosphorylates SCG10 and targets it for degradation, then JNK inhibition should preferentially preserve nonphosphorylated, lower-molecular-weight SCG10, and protease inhibition should preserve phosphorylated, more slowly migrating SCG10 species. Consistent with these expectations, we find that treatment with SP600125 preferentially preserves lower-molecular-weight SCG10 species. In contrast, treatment with the proteasome inhibitor MG132 preferentially preserves higher-molecular-weight (phosphorylated) SCG10 species (Fig. 3*A*). To confirm that the higher-molecular-weight SCG10 species preserved by MG132 represent phosphorylated forms, we treated these protein lysates with calf intestinal phosphatase. Following phosphatase treatment, the SCG10 species that remained were the lower-molecular-weight forms (Fig. 3*B*), demonstrating that phosphorylated SCG10 species accumulate when degradation is inhibited.

As an independent test of whether JNK phosphorylation of SCG10 promotes its degradation, we mutated the two known JNK phosphorylation sites on SCG10 (serines 62 and 73) (22) to alanines (a mutation termed "SCG10-AA"). Using lentivirus, we expressed Venus-tagged WT (ven-SCG10) and mutant SCG10 (ven-SCG10-AA) in DRG neurons and examined the degradation of mutant SCG10 6 h after axotomy. Using the Venus tag, we were able to distinguish lentivirally expressed SCG10 from endogenous SCG10 and therefore could monitor their loss independently. We found that after axotomy the loss of mutant ven-SCG10 was significantly less than that of WT ven-SCG10 [45 ± 14% ven-SCG10 vs. 88 ± 21% ven-SCG10-AA remaining at 6 h postaxotomy (mean ± SEM); $n = 3$; $P < 0.05$ by paired t test] (Fig. 3*C*). Similar results were observed with nontagged SCG10 constructs (see below). These results demonstrate that the two serine sites are required for rapid SCG10 turnover and support a model wherein JNK phosphorylation at Ser62 and Ser73 targets SCG10 for degradation.

In addition, we found that JNK also promotes SCG10 turnover in a Ser62/Ser73-independent manner. Degradation of ven-SCG10-AA was attenuated further after SP600125 treatment [19 ± 6% ven-SCG10-AA remaining with vehicle treatment vs. 53 ± 5% ven-SCG10-AA remaining with SP600125 treatment at 12 h postaxotomy (mean ± SEM); $n = 3$; $P < 0.005$] (Fig. 3*D*), indicating that phosphorylation at Ser62 and Ser73 is not the only mechanism by which JNK regulates stability of SCG10. The additional mechanism may involve direct phosphorylation by JNK on other sites of SCG10 or indirect regulation of SCG10. Hence, JNK targets SCG10 for degradation via both Ser62/Ser73 phosphorylation-dependent and independent mechanisms.

SCG10 Is Transported Anterogradely in Axons. To test the hypothesis that SCG10 level is maintained in healthy axons by continuous delivery of newly synthesized protein from the cell body, we examined axonal transport of SCG10. DRG neurons were infected with lentivirus expressing ven-SCG10, and the rate of ven-SCG10 axonal transport was analyzed by live imaging. We found that ven-SCG10 undergoes anterograde transport with an average velocity of 1.16 ± 0.11 μm/s (mean ± SEM; $n = 10$) (Fig. 4 and Movie S1). Anterograde transport of SCG10 predominated over retrograde transport, with anterograde accounting for 83 ± 3% of transport compared with retrograde transport that accounts for 17 ± 3% (mean ± SEM; $n = 9$; $P < 0.001$). These results demonstrate that SCG10 proteins in the axon are replenished continuously by transport from the cell body. An interruption of fast axonal transport, such as occurs after axon transection, in the face of sustained basal SCG10 degradation would lead to the observed selective loss of SCG10 in the distal axon segments. Similarly, continued SCG10 axonal transport proximal to the injury site would lead to the observed accumulation of SCG10 in proximal axon stumps (Fig. 1*D*).

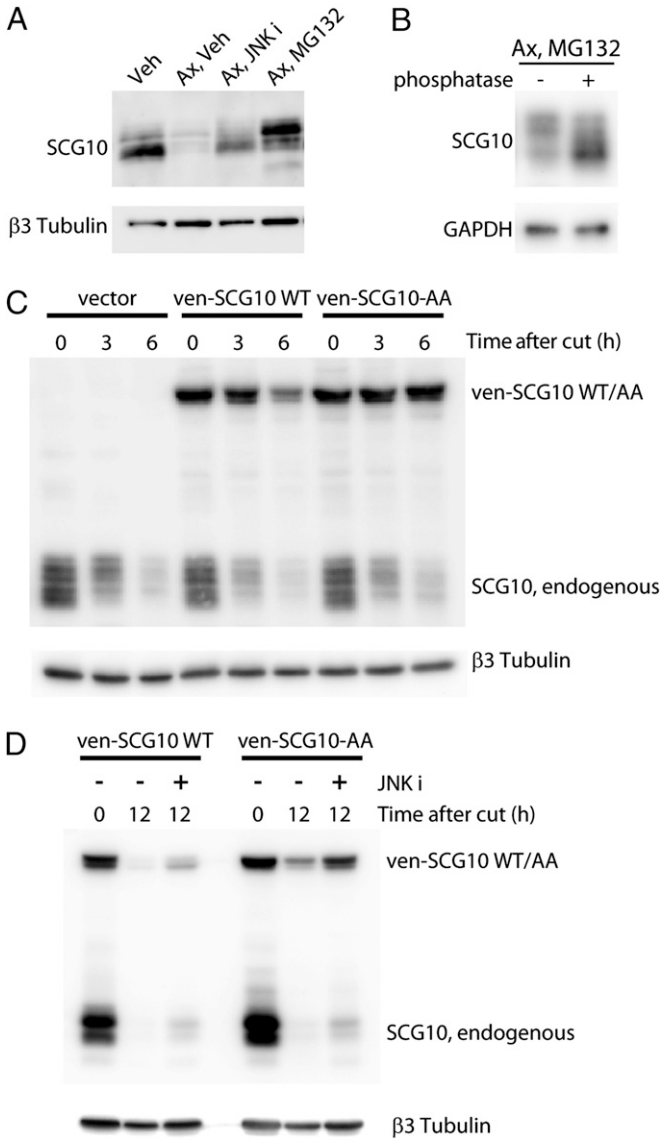

Fig. 3. JNK phosphorylation targets SCG10 for proteasomal degradation. (*A*) DRG cultures were axotomized (ax) and treated with DMSO (veh), 15 μM SP600125 (JNK i), or 20 μM MG132 for 3 h, and the distal axons were subjected to Western blot analysis to assess the gel mobility of SCG10. SP600125-treated axons preferentially preserve lower-molecular-weight SCG10, whereas MG132-treated axons preferentially preserve the higher-molecular-weight form. β3 tubulin is shown as a loading control. (*B*) In vitro treatment with phosphatase shows that the higher-molecular-weight SCG10 species accumulated by MG132 treatment is phosphorylated SCG10. Axonal extracts were obtained from the cultures that were axotomized, treated with MG132 for 3 h, and subsequently incubated with calf intestinal phosphatase. The amounts of GAPDH show equal loading. (*C*) The axonal levels of lentivirally expressed ven-SCG10 WT and ven-SCG10-AA were assayed after axotomy. Immunoblot with anti-SCG10 antibody shows both endogenous and lentivirally expressed ven-SCG10 (*Upper*). Ven-SCG10 WT is lost significantly in the distal axons by 6 h after axotomy, whereas ven-SCG10-AA is largely preserved. β3 tubulin is shown as a loading control (*Lower*). (*D*) JNK inhibition by 15 μM SP600125 (JNK i) attenuates the degradation of both wild-type SCG10 (ven-SCG10 WT) and alanine-mutant SCG10 (ven-SCG10-AA) after axotomy (*Upper*). β3 tubulin is shown as a loading control (*Lower*).

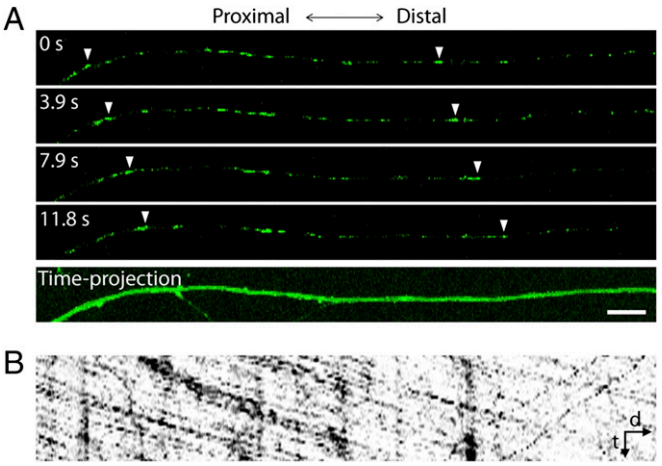

Fig. 4. Anterograde axonal transport of SCG10. (*A*) Live imaging of Venus-tagged SCG10 in cultured DRG axons. (*Upper*) Four single frames with the same time interval are shown as representative images. Arrowhead indicates tracking of ven-SCG10 puncta. (*Lower*) The axon is visualized by maximum projection of all single frames in the time-lapse images. (Scale bar, 10 μm.) (*B*) A kymograph generated from the axon shown in *A* demonstrates that ven-SCG10 is transported predominantly in the anterograde direction. The kymograph corresponds to a 79-s live imaging. d, distance; t, time.

Knockdown of SCG10 Accelerates Axon Degeneration After Injury. SCG10 is lost selectively in distal axon segments and precedes axonal fragmentation. These findings led us to test the hypothesis that SCG10 may be important for axonal maintenance. To test the requirement of SCG10 for axonal survival, we used lentivirus to express shRNAs targeting SCG10 in DRG neurons. Because prolonged SCG10 shRNA expression led to neuronal apoptosis, we also lentivirally expressed Bcl-xl, an inhibitor of neuronal apoptosis (27). Bcl-xl expression preserves neuronal viability without affecting axonal degeneration after axotomy (Fig. 5) (28, 29). Three different shRNA constructs efficiently reduced SCG10 protein levels (Fig. 5*B*). This loss of SCG10 is not sufficient to trigger axonal degeneration (Fig. 5*C*). Next, we set out to determine whether the absence of SCG10 promotes axonal degeneration when degeneration is triggered by axotomy. Axonal degeneration was quantified via the "degeneration index," a measure of fragmented axonal area calculated from phase-contrast images (28, 30). In neurons infected with control virus, axonal fragmentation is apparent by 6 h after transection and is robust by 9 h after axotomy (Fig. 5*C*). In contrast, following knockdown of SCG10, degeneration is largely complete by 6 h after axotomy (Fig. 5 *A* and *C*). All three shRNA constructs targeting SCG10 induced this acceleration of axon degeneration ($P < 0.001$ at 6 h). This phenotype is rescued when we restore SCG10 protein levels by expressing a rat SCG10 cDNA that is resistant to shRNA no. 1 ($P < 0.01$) (Fig. 5). Rescue demonstrates that the accelerated axon degeneration phenotype of shRNA no. 1 is caused by the knockdown of SCG10 rather than by an off-target effect of the shRNA. Collectively, these results demonstrate that SCG10 is functionally important for axonal maintenance after axotomy. SCG10 loss is not the trigger for axonal degeneration but rather may be a permissive factor that allows activated degeneration pathways to initiate axon destruction.

Maintaining SCG10 Levels After Injury Delays Axonal Degeneration. If SCG10 loss in the early postaxotomy period is permissive for the onset of axonal fragmentation, then experimentally maintaining SCG10 levels in injured axons should delay axonal degeneration. To test this hypothesis, we used lentivirus to express the SCG10 with mutated JNK phosphorylation sites (SCG10-AA) (Fig. 3*C*). We expressed nontagged forms of wild-type SCG10 and mutant SCG10-AA to avoid any potential confounds from the Venus tag. Total axonal SCG10 levels were analyzed by Western blot using anti-SCG10 antibody that detects both endogenous and exogenous SCG10 proteins. We confirmed that lentivirus-expressed wild-type SCG10 is degraded rapidly after axotomy, but SCG10-AA is more stable ($P < 0.05$, SCG10 WT vs. SCG10-AA at 6 h postaxotomy) (Fig. 6 *A* and *B*). At 6 h postaxotomy, axons expressing stabilized SCG10-AA had total SCG10 levels similar to the levels of en-

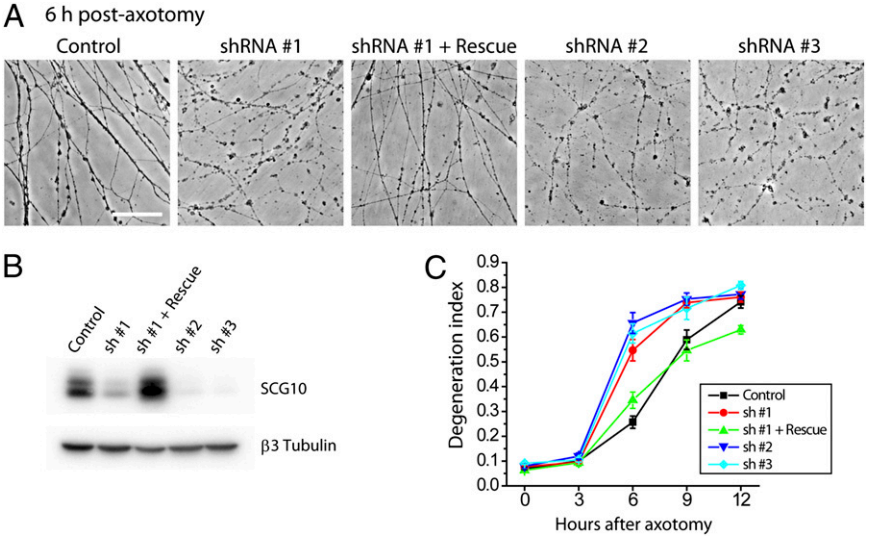

Fig. 5. Knockdown of SCG10 accelerates axon degeneration after injury. (*A*) SCG10 was depleted by lentiviral expression of three different shRNA constructs (shRNA nos. 1, 2, and 3). SCG10 expression was restored by coexpressing rat SCG10 cDNA with the mouse-specific shRNA no. 1. Phase-contrast images show that axonal fragmentation is robust at 6 h after axotomy when SCG10 is knocked down; however, this effect is diminished when SCG10 expression is rescued. (Scale bar, 500 μm.) (*B*) Immunoblot for SCG10 shows effective knockdown of SCG10 by the lentiviral shRNAs and the rescue of the protein expression. β3 tubulin is shown as a loading control. (*C*) Quantification of the results in *A*. The degeneration index is a measure for fragmented axons. By ANOVA at 6 h, $P < 0.001$ for control vs. shRNA no. 1, 2, or 3; $P < 0.01$ for shRNA no. 1 vs. shRNA no. 1 + rescue. At 9 h, $P < 0.05$ for control vs. shRNA no. 1 or 2; $P < 0.01$ for, shRNA no. 1 vs. shRNA no. 1 + rescue. n = 9–15. Error bars represent SEM.

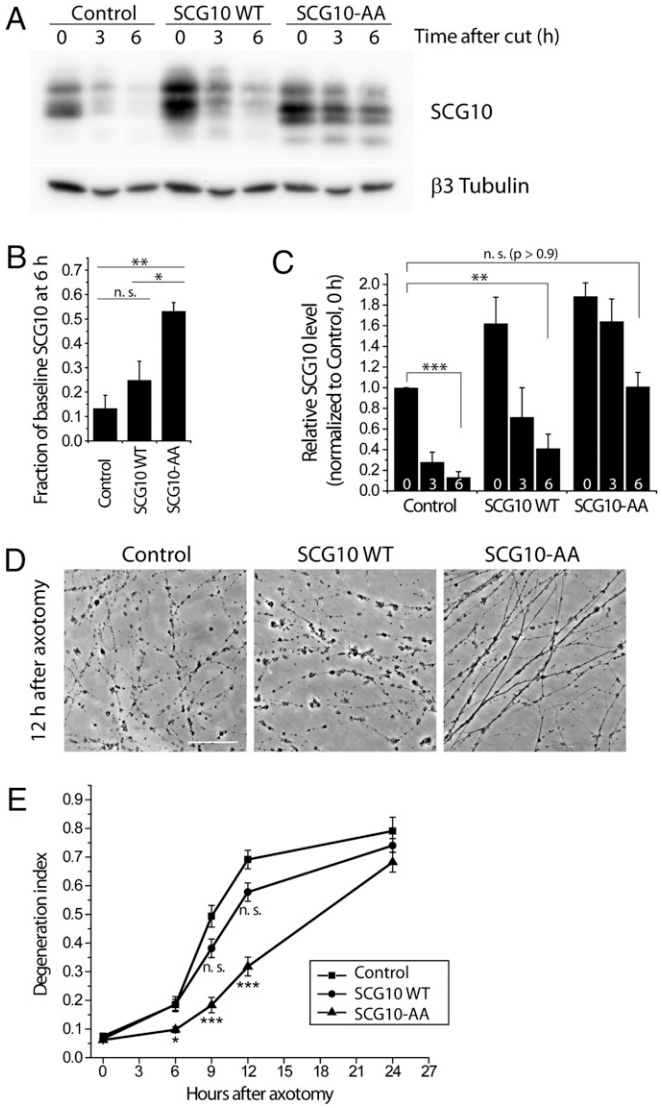

Fig. 6. Shielding SCG10 from JNK phosphorylation delays axonal degeneration. (*A*) Axonal SCG10 levels were assayed with the lentiviral expression of control vector, nontagged SCG10 WT, or nontagged SCG10-AA following axotomy. Immunoblot for SCG10 shows that the level of lentivirally expressed SCG10 WT is decreased greatly by 6 h after axotomy, whereas SCG10-AA is largely preserved. β3 tubulin is shown as a loading control. (*B*) Quantification of the results in *A*. The levels of SCG10 at 6 h after axotomy are quantified as the fraction of the baseline SCG10 level (0 h after cut) in the respective lentiviral infection. Control, $n = 4$; SCG10 WT and SCG10-AA, $n = 3$; $^{*}P < 0.05$, $^{**}P < 0.005$ by ANOVA. Error bars represent SEM. (*C*) Results from *A* were quantified as relative levels of SCG10 normalized to that in the control at 0 h after cut. Numbers at the bottom of the bars represent time (in hours) after axotomy. Lentiviral expression of SCG10-AA leads to the preservation of SCG10 comparable to the level of endogenous SCG10 in unaxotomized axons up to 6 h after axotomy. Control, $n = 4$; SCG10 WT and SCG10-AA, $n = 3$; $^{**}P < 0.005$, $^{***}P < 0.001$ by *t* test. Error bars represent SEM. (*D*) Phase-contrast images of axons were taken 12 h after axotomy from the DRG cultures infected with the indicated lentiviruses. Expression of SCG10-AA attenuates axon fragmentation. (Scale bar, 500 μm.) (*E*) Degeneration indices were obtained from the results in *D* and plotted against time after axotomy. At 0, 6, and 9 h after axotomy, $n = 15$–18; 12 h after axotomy, $n = 10$–12; 24 h after axotomy, $n = 5$–6; $^{*}P < 0.05$, $^{***}P < 0.001$ vs. control lentivirus by ANOVA. Error bars represent SEM. n.s., not significant.

dogenous SCG10 in uninjured axons ($P > 0.9$) (Fig. 6*C*). In contrast, lentiviral expression of wild-type SCG10 cannot maintain high levels of protein after axotomy; 6 h after axotomy, the total SCG10 levels were significantly lower than the levels of endogenous SCG10 in uninjured axons ($P < 0.005$) (Fig. 6*C*). These differences in the maintenance of SCG10 levels after axonal injury had important functional consequences. The expression of the more labile wild-type SCG10 had no effect on the rate of axonal degeneration. In contrast, expression of stabilized SCG10-AA significantly delayed axonal degeneration ($P < 0.001$ at 9 and 12 h) (Fig. 6 *D* and *E*). Therefore, adequate levels of SCG10 in injured axons protect axons from fragmentation.

The alanine mutations at Ser62 and Ser73 on SCG10 do not fully block degradation of the protein after axotomy (Fig. 3*D*), and axons expressing SCG10-AA become fragmented by 24 h after axotomy (Fig. 6*E*). If SCG10 loss were a permissive signal for execution of axon degeneration, then axons should be protected longer if SCG10 levels were maintained longer. Inhibiting JNK activity leads to prolonged preservation of SCG10-AA after axotomy (Fig. 3*D*), so we tested whether inhibiting JNK while expressing SCG10-AA would protect axons to a greater extent than either SCG10-AA expression or JNK inhibitors alone. As observed with the Venus-tagged form of SCG10-AA (Fig. 3*D*), JNK inhibition by SP600125 reduces the loss of nontagged SCG10-AA after axotomy, maintaining axonal SCG10 levels at 9 h postaxotomy similar to the levels observed in uninjured control axons ($P > 0.6$) (Fig. 7 *A* and *B*). As predicted, inhibiting JNK significantly enhanced the axonal protection conferred by SCG10-AA overexpression. At 24 h postinjury, there is little protection from either JNK inhibition or SCG10-AA expression alone, but simultaneously inhibiting JNK and expressing SCG10-AA is strongly axoprotective ($P < 0.001$) (Fig. 7 *C* and *D*). The correlation between the persistence of SCG10 protein and the efficacy of axoprotection is a further indication that loss of SCG10 is permissive for axon loss.

Expressing SCG10-AA Preserves Mitochondrial Transport in Injured Axons. We next investigated the mechanisms by which maintaining SCG10 levels protects injured axons from degeneration. Axonal injury disrupts axonal transport of cargoes along microtubules, some of which are important for axonal maintenance (31). For example, mitochondria are trafficked by axonal transport, and disruption of such transport is associated with axonal degeneration (32). In healthy axons, SCG10 regulates microtubule dynamics that in turn affect the efficacy of axon transport (33). Therefore, we hypothesized that SCG10 loss after injury may contribute to axon degeneration by impairing microtubule-dependent transport of essential cargoes such as mitochondria. We tested whether preserving SCG10 after injury helps maintain mitochondrial transport by expressing SCG10-AA and monitoring the movement of fluorescently labeled mitochondria. The number of mitochondria moving along axons was counted to obtain the percent of motile mitochondria. Before axotomy, the percent of motile mitochondria is indistinguishable between axons expressing SCG10-AA and those infected with control virus. In the control axons, axotomy dramatically disrupts mitochondrial transport, resulting in an approximately threefold reduction in the percent of motile mitochondria at 1 h postaxotomy ($P < 0.001$) (Fig. 8). However, in axons expressing SCG10-AA, mitochondrial movement is significantly maintained ($P < 0.05$; control and axotomy vs. SCG10-AA and axotomy) (Fig. 8). Importantly, this observation was made early after injury (1 h postaxotomy), so it is unlikely that the transport deficit was caused by axonal fragmentation. Instead, these results are consistent with a model in which preserving SCG10 retains mitochondrial motility after injury, and maintaining mitochondrial motility is a potential mechanism of axoprotection (34).

Discussion

Axonal degeneration is a major cause of neurological disability. Although the precise mechanism of axon loss is poorly understood, it is clear that axons are dismantled by a carefully orchestrated mechanism. Proteasome activity contributes to axon

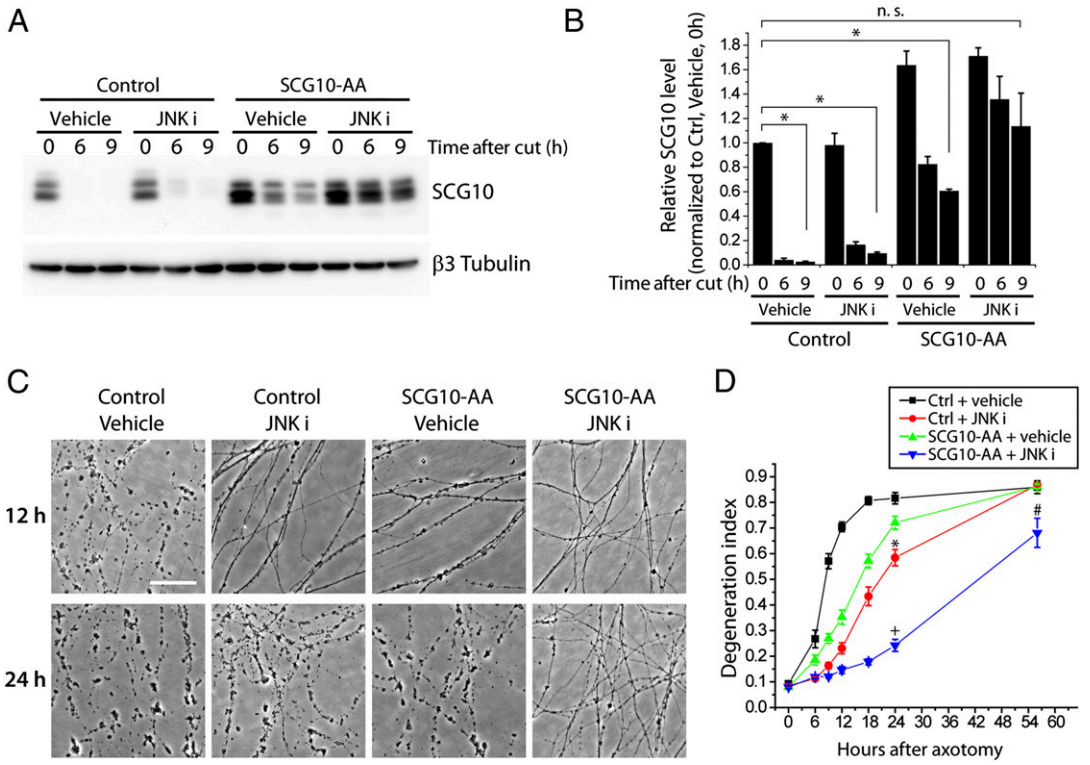

Fig. 7. Axonal protection by expression of SCG10-AA is enhanced by JNK inhibition. (*A*) Axonal SCG10 levels were assayed with the lentiviral expression of control vector or nontagged SCG10-AA after axotomy with or without treatment of JNK inhibitor, 15 μM SP600125 (JNK i). Immunoblot with anti-SCG10 antibody shows that the levels of total SCG10 are maintained longer in the axons treated with JNK inhibitor. β3 tubulin is shown as a loading control. (*B*) Results in *A* are quantified as relative SCG10 levels normalized to the basal SCG10 level (control, vehicle-treated, 0 h after cut). $n = 3$; $^{*}P < 0.001$ by ANOVA. Error bars represent SEM. (*C*) Axonal protection is extended by expressing SCG10-AA and inhibiting JNK activity. Axons are fragmented by 24 h after axotomy when treated with either lentiviral expression of SCG10-AA or JNK inhibitor. In contrast, simultaneously expressing SCG10-AA and inhibiting JNK leads to significant axonal preservation. (Scale bar, 500 μm.) (*D*) Quantification of the results in *C*; 0–24 h, $n = 12$; 56 h. $n = 3$ for control and vehicle; $n = 8$ for other conditions. Statistical significance is noted only for 24 h and 56 h after axotomy; by ANOVA, $^{*}P < 0.001$ vs. control and vehicle; $^{+}P < 0.001$ vs. control and vehicle, vs. control and JNK inhibitor and vs. SCG10-AA and vehicle; $^{\#}P < 0.05$ vs. control and vehicle; $^{\#}P < 0.01$ vs. control and JNK inhibitor and vs. SCG10-AA and vehicle. Error bars represent SEM.

breakdown (11), likely by promoting the degradation of factors that are required for axonal maintenance after injury. Degradation of specific maintenance factors may stimulate the activation of axonal degeneration cascades. NMNAT2 is an axonal-survival factor, and depletion of NMNAT2 triggers degeneration of uninjured axons (12). On the other hand, additional maintenance factors may function in the injured axons to establish a set point at which injury-induced degeneration pathways are engaged. Loss of such limiting factors would allow active degeneration pathways to execute axonal destruction. Elucidating the identity and regulation of such axonal-maintenance factors may lead to novel axoprotective therapeutic strategies.

Degeneration of injured axons is regulated by many kinase pathways, including those involving DLK, JNK, GSK3β, and IκB kinase (16, 21, 28, 35). Within the first few hours after axonal damage, before morphological signs of degeneration, these pathways act to promote subsequent axonal fragmentation. Despite their functional importance, substrates of these kinase pathways in the injured axon remain mostly unknown. Here we tested the hypothesis that JNK targets SCG10, a protein involved in microtubule dynamics, in the axonal degeneration pathway. SCG10 is degraded rapidly after injury both in cultured DRG neurons and in vivo in adult sciatic nerve. The JNK phosphorylation sites on SCG10, serines 62 and 73, are required for rapid SCG10 degradation, and treatment with a JNK inhibitor preferentially preserves rapidly migrating, hypophosphorylated SCG10 species. In contrast, treatment with a proteasome inhibitor after axonal injury preferentially preserves the more slowly migrating, phosphorylated forms of SCG10. Thus, JNK phosphorylation of SCG10 likely targets SCG10 for degradation, consistent with the phosphorylation-dependence of substrate recognition by degradation machinery (36).

After transection of peripheral axons, distal axon segments degenerate, but proximal axons are spared and often regenerate. Interestingly, we found that SCG10 is lost in axon segments distal to the site of transection but is not lost in proximal axon stumps even though the distal and proximal segments receive identical initial trauma. SCG10 loss appears to be an early and selective marker of axons destined to degenerate. Such markers could be useful diagnostically to identify unhealthy axons before irreversible fragmentation occurs.

How is SCG10 lost selectively in distal axon segments and spared in proximal segments? One possibility is that the SCG10 degradation signal is activated selectively in the distal segment. Alternatively, SCG10 may be degraded rapidly in healthy axons and replenished by axonal transport. In this model, any injury that blocks transport would lead to selective and rapid SCG10 degradation distal to the injury. Our data support this second model, because we found similar turnover of SCG10 in intact and injured axons, and treatment with JNK inhibitor increased SCG10 levels in both healthy and damaged axons. Consistent with this observation, inhibiting protein synthesis in uninjured neurons results in rapid SCG10 loss in axons, and JNK inhibition slows the rate of SCG10 loss. Furthermore, SCG10 undergoes rapid axonal transport in healthy axons. Thus, SCG10 is degraded rapidly in healthy axons and is replenished by de novo synthesis and axonal transport from cell bodies. Our results are consistent with reports that SCG10 is lost in neuronal cell lines after treatment with taxol (37),

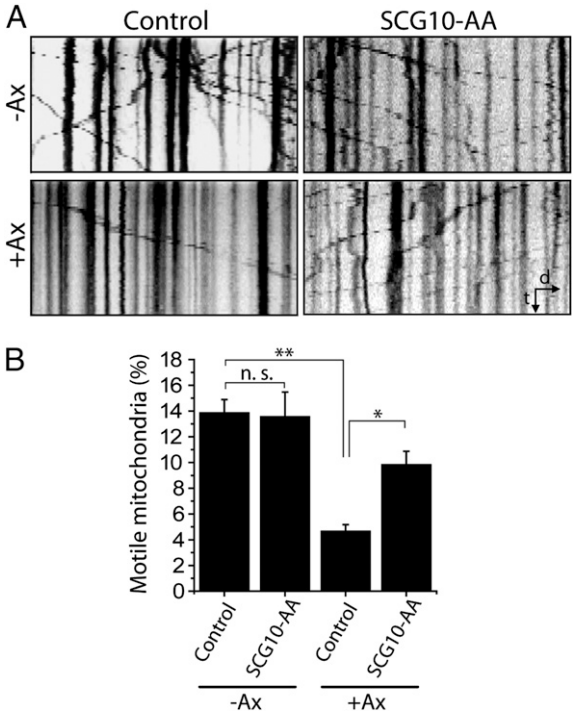

Fig. 8. Mitochondrial transport is preserved by the expression of SCG10-AA. (*A*) Kymographs showing axonal transport of mitochondria labeled with mitochondrially targeted DsRed before axotomy (−Ax) or 1 h after axotomy (+Ax). The number of motile mitochondria decreases markedly after injury in control (vector-expressing) axons, whereas axons expressing SCG10-AA largely maintain mitochondrial transport. The kymographs correspond to 5 min of live imaging. Distal is to the right. d, distance; t, time. (*B*) Percent of motile mitochondria shown in *A* is quantified. $n = 13–14$; $^{*}P < 0.05$, $^{**}P < 0.001$ by ANOVA. Error bars represent SEM. n.s., not significant.

a potent disruptor of axonal transport. In sum, our data show that SCG10 is a labile axonal protein whose rapid degradation is dependent in part on JNK phosphorylation. The interruption of SCG10 replenishment after axonal injury in the face of continued JNK-regulated targeting of SCG10 for degradation results in SCG10 loss in distal axon segments after injury.

The accumulation of SCG10 in the proximal axonal stump after transection follows naturally from our model. Other studies have also found that SCG10 levels are increased proximal to the site of traumatic injury in both the central and peripheral nervous systems (38–40). This SCG10 accumulation in the end bulbs of the proximal stump may be functionally important for axonal regeneration, because SCG10 within growth cones encourages the outgrowth of developing axons (23, 41–43). Of note, increased levels of SCG10 correlate closely with axon regeneration and sprouting after axon severing and ischemic brain injury (44–46). Thus, regulation of SCG10 turnover and rapid axonal transport may coordinate distal axonal degeneration and proximal axonal regeneration after injury.

Our data show that SCG10 loss is functionally important. We found that removing SCG10 significantly accelerates the degeneration of transected axons. Therefore, SCG10 helps control the extent of the lag in the early postinjury period when little fragmentation is observed in the distal axons. Interestingly, depriving SCG10 does not lead to axonal degeneration. In contrast, knockdown of NMNAT2, another labile axonal protein important for axonal degeneration, directly triggers degeneration (12). Our data suggest that SCG10 loss is not a trigger for degeneration but rather is a permissive signal that enables an orchestrated series of injury responses to promote rapid axonal degeneration.

To determine if maintaining SCG10 levels could delay axonal degeneration, we directly preserved SCG10 levels after axonal injury by expressing a mutant SCG10 in which two JNK phosphorylation sites (serines 62 and 73) were replaced by alanines. Using this more stable SCG10 mutant, we found that preserving SCG10 levels could delay axon fragmentation significantly. Thus, maintaining adequate levels of SCG10 is sufficient to stabilize axons. Notably, axons were not protected by the overexpression of WT SCG10 that can be phosphorylated by JNK and degraded rapidly, providing a direct link between JNK phosphorylation of SCG10 and its role in axonal degeneration. In addition, pharmacologically inhibiting JNK activity further slows the degradation of the mutant SCG10, demonstrating that JNK promotes the degradation of SCG10 through other mechanisms, in addition to the phosphorylation of serines 62 and 73. Treatment with JNK inhibitor in conjunction with the expression of the alanine-mutant SCG10 leads to a further delay in axonal degeneration, perhaps reflecting additional functions of JNK inhibition. However, the ability of JNK inhibition both to extend the life of SCG10-AA and to delay axon degeneration is consistent with the model that loss of SCG10 is required for the execution of axonal degeneration. Hence, understanding the mechanisms regulating SCG10 stability may lead to methods for attenuating axonal destruction, for example, by inhibiting specific degradation machinery targeting SCG10.

SCG10 regulates microtubule dynamicity, and this regulation may be important for its role in axonal maintenance. Microtubules normally undergo transitions between polymerization and depolymerization, a property referred as "dynamic instability." SCG10 binds tubulin heterodimers, bending them and pushing the equilibrium of microtubule dynamic instability toward disassembly (23). During development SCG10 is required for axonal microtubules to be sufficiently dynamic to sustain axon outgrowth. When SCG10 levels are decreased, microtubule dynamism dwindles, and neurite outgrowth is restricted (41, 42). Excessive microtubule stability also disrupts adult axons: Pharmacological microtubule stabilizers such as taxol induce axonal degeneration (47) and cause neuropathy in patients (48). Furthermore, we have demonstrated that loss of *Drosophila* stathmin, an SCG10 ortholog, leads to axon terminal retraction at the neuromuscular junction (49). Thus, rapid loss of SCG10 following injury may promote axonal degeneration by impairing microtubule dynamics. Likewise, maintaining SCG10 levels by overexpression may protect axons by retaining sufficient dynamic instability.

Microtubule misregulation may contribute to axon deterioration by impairing axonal cargo transport. Both aberrant stabilization and destabilization of microtubules are implicated in the pathogenesis of neurodegenerative diseases such as Huntington disease and hereditary spastic paraplegia, in which altered microtubule dynamics disrupt motor protein–microtubule interaction (33). Mitochondria are an axon transport cargo essential for axonal integrity; defective mitochondrial transport is a common feature of many neurodegenerative diseases (32). Consistent with this model, we found that axotomy leads to a rapid decline in mitochondrial transport in distal axons, whereas maintaining SCG10 levels preserves mitochondrial trafficking following axotomy. Interestingly, expression of the axoprotective molecule Wld^{S} also preserves mitochondrial motility (34), suggesting that retaining mitochondrial transport may be a fundamental mechanism for maintaining injured axons.

In conclusion, our data indicate that SCG10 is a labile protein whose presence in the axonal compartment signals a healthy connection with the cell body, that SCG10 is an axonal-maintenance factor that promotes mitochondrial motility, and that SCG10 loss is permissive for execution of the axonal degeneration program following injury.

Materials and Methods

DNA Constructs. A plasmid encoding cytoplasmically targeted Nmnat1 has been described previously (25). Rat SCG10 cDNA were kindly provided by

E. T. Coffey (Turku Centre for Biotechnology, Turku, Finland) (22). Site-directed mutagenesis was used to create SCG10-AA from wild-type SCG10. For lentiviral expression of nontagged SCG10 proteins, wild-type SCG10 and SCG10-AA were cloned into FCIV vector with an internal ribosome entry site (IRES)-enhanced YFP (Venus) cassette that labels infected cells as described previously (5). To generate Venus-tagged SCG10 constructs, the IRES sequence was removed from the FCIV vector, and the Venus sequence was ligated to the C terminus of the SCG10 coding sequence by PCR cloning strategies. The Bcl-xl lentivirus construct was described by Vohra et al. (29). shRNA constructs for SCG10 were purchased from Open Biosystems (catalog nos. RMM4431-98755925, 101260727, and 101265301).

Mouse DRG Spot Culture Preparation and Treatment. Embryonic DRG cultures were made as described previously by Miller et al. (16). Briefly, we cultured DRGs from embryonic day (E) 12.5–13.5 CD1 mice (Charles River) in poly-D-lysine- (Sigma) and laminin- (Sigma) coated 24-well plates (Corning). Collected DRGs were trypsinized for 20 min at 37 °C, triturated in medium, and plated as a spot at a density of approximately two DRGs per well in 2 μL medium. The plates were incubated for 20 min at 37 °C to attach cells to the plastic, followed by the addition of Neurobasal medium (Invitrogen) supplemented with 2% (vol/vol) B27 (Invitrogen), 25 ng/mL nerve growth factor (Harlan Bioproducts), and 1 μM 5-fluoro-2′-deoxyuridine and 1 μM uridine (Sigma) to block cell division of nonneuronal cells. Cultures were maintained for 8–9 d before axotomy or drug treatment, so that axons were allowed to grow away from the spot where the cell bodies were placed. Axons at this stage (DIV 8–9) degenerated more rapidly (Fig. 5) than axons grown for 2 wk (16), as observed consistently in different conditions including control and JNK inhibitor-treated cultures. We axotomized neurons using a microscalpel. We used SP600125 (Sigma) at 15 μM and MG132 (Sigma) at 20 μM and treated the control wells with DMSO, which was used as vehicle.

Lentivirus Infection. Lentiviruses were generated as described previously (5). We added lentivirus to the culture at DIV 4–5 and allowed 4–5 d for expression. SCG10 shRNA viruses were added at DIV 1–2 for efficient knockdown. To confirm efficient overexpression or knockdown of a gene, we monitored fluorescence from Venus and performed Western blot analysis to assess the level of the protein of interest.

Mouse in Vivo Sciatic Nerve Transection. We used adult C57BL6/J mice (Jackson Laboratory). We anesthetized animals, made a small incision unilaterally to expose the sciatic nerve, transected the sciatic nerve with surgical scissors, and then sutured the incision. Three hours after transection, mice were euthanized by CO_2, and the sciatic nerves were removed for Western blot analysis. From the transected nerve, only distal segments were collected. Mouse experiments were performed under the supervision of Division of Comparative Medicine at Washington University.

Western Blot. To make axon-only lysates in vitro, we cut around the neuronal cell bodies using a microscalpel and removed the cell bodies with forceps. Then the remaining axon compartment was lysed in Laemmli buffer. For in vivo analysis, sciatic nerves were homogenized in lysis buffer [20 mM Tris·HCl (pH 7.5,) 150 mM NaCl, 1 mM Na_2EDTA, 1 mM EGTA, 1% Triton X-100, 2.5 mM sodium pyrophosphate, 1 mM β-glycerophosphate, 1 mM Na_3VO_4] with protease inhibitor mixture (Roche). Western blot analyses were performed following standard protocols. The following primary antibodies were used: anti-SCG10 (Proteintech Group), anti-β3 tubulin (Tuj1; Covance), and anti-GAPDH (Millipore). To assay protein levels, intensities of protein bands were measured by Quantity One software (Bio-Rad), and SCG10 levels were normalized by comparison with the loading control.

Protein Turnover Assay. Protein turnover was examined exclusively in the axonal compartment. Cultured DRG neurons were treated with CHX (Sigma) at 100 μg/mL to block protein synthesis for the indicated time. For JNK inhibition, SP600125 (Sigma) was used at 15 μM. Axonal lysates were prepared as described above and used for Western blot analysis. The turnover of SCG10 loss was calculated using the curve-fitting algorithm in Origin software (OriginLab). R^2 values for fitted curves were larger than 0.95 in every condition.

Protein Dephosphorylation. Embryonic DRG explants (E14.5–15.5) were cultured with the method used for DRG spots. After 8 DIV, a microscalpel was used to separate cell bodies from axons. The axons were collected, resuspended in 50 μL ice-cold NEB3 buffer (New England BioLabs) containing protease inhibitor (Complete-Mini; Roche), and lysed by vortexing three times. Lysates were incubated at 37 °C with 10 μL of calf intestinal phosphatase (New England BioLabs) for 1 h. Control axons were processed in parallel, in the presence of phosphatase inhibitor mixture 2 and 3 (Sigma). For Western blot analysis, samples were lysed further by adding 5 μL of 10% (wt/vol) SDS, vortexing, incubation on ice for 10 min, and boiling at 100 °C for 10 min. Western blot was performed as described.

Immunofluorescence. DRG neurons were cultured on four-well slide dishes (Lab-Tek, Thermo Scientific) for high-quality fluorescence microscopy. Neurons were fixed in 4% (wt/vol) paraformaldehyde. After one washing in PBS and another washing in PBS with 0.1% Triton X-100 (PBS-T), samples were blocked in blocking solution [5% (vol/vol) normal goat serum in PBS-T] at room temperature and then were incubated with primary antibodies diluted in blocking solution overnight at 4 °C. Cultures then were washed two times with PBS-T, incubated with secondary antibodies in blocking solution for 1 h at room temperature, washed three times in PBS-T, and mounted in VectaShield (Vector Laboratories). Anti-SCG10 C-terminal rabbit antibodies were kindly provided by A. Sobel (Institut National de la Santé et de la Recherche Médicale, Paris) (50), and we also created antibodies against the same peptide sequence for immunostaining. Anti-β3 tubulin antibodies (Tuj1) were purchased from Covance. Alexa Fluor 488-conjugated anti-mouse secondary antibody (Invitrogen) and Cy3-conjugated anti-rabbit secondary antibody (Jackson ImmunoResearch) were used at 1:1,000–1:500.

Confocal Imaging and Quantification of Protein Level. Samples were imaged with a Nikon D-Eclipse C1 confocal microscope using a 20× oil objective. Images shown are z projections of confocal stacks acquired from serial laser scanning. The axonal SCG10 level was assessed by using Metamorph software (Molecular Devices). First, images were thresholded for β3 tubulin immunoreactivity to define the axonal area. Then, the average SCG10 intensity was obtained by measuring SCG10 immunofluorescence within the defined axonal area in each image.

Live Imaging. DRG neurons were plated on poly-L-lysine/laminin-coated glass-bottomed dishes (World Precision Instruments). Venus-SCG10 was expressed by lentivirus infection on DIV 1–2. After 3 d, the cultures were mounted on a confocal microscope chamber (LSM510M; Zeiss) at 37 °C and 5% CO_2 atmosphere. Live images were acquired using Apochromat 40× objective. To assess axon transport, maximum time-projection images and kymographs were obtained by ImageJ (National Institutes of Health). We calculated the velocity of moving particles from the slope of streaks in kymographs. The ratio of anterogradely transported particles to retrogradely transported particles was obtained from each axon by counting the number of streaks representing each direction from 5-min-long kymograph. Mitochondrial movement was imaged and quantified as follows. Control FCIV vector or nontagged SCG10-AA mutant was coexpressed with mitochondrially targeted DsRed using lentivirus infection on DIV 4. At DIV 7–8, culture plates were mounted on a microscope stage (Eclipse TE-2000E; Nikon) maintained at 37 °C. Moving mitochondria were monitored with a 20× objective 500 μm from the axotomy site. Images were acquired every 5 s for 5 min. Kymographs were made from four 100-μm axon segments randomly selected from each movie by using ImageJ.

Phase-Contrast Imaging and Quantifying Axon Degeneration in Vitro. Axon degeneration was analyzed as described previously (16). Briefly, phase-contrast images were obtained on an inverted light microscope (CKX41; Olympus) with a 20× objective. Three nonoverlapping images of each well were taken at each time point and were assessed for axon degeneration. Images were processed with the auto-level function in Photoshop (Adobe) for brightness adjustment. We then analyzed the images by using a macro written in ImageJ to calculate the degeneration index (28, 30). After images were binarized, the total axon area was defined by the total number of detected pixels. The area of degenerated axon fragments was calculated using the particle analyzer function. To calculate the degeneration index, we divided the area covered by axon fragments by the total axon area. We averaged the indices of three images taken from the same well to calculate the mean degeneration index for each well. Degeneration studies were performed in at least three independent experiments.

Statistical Analysis. A Student *t* test or ANOVA was used to test statistical significance. When the *t* test was used, an independent *t* test was performed unless paired tests are indicated. When ANOVA was used, a Tukey posttest was performed for means comparison. *P* values >0.05 were considered not significant.

ACKNOWLEDGMENTS. We thank Dr. A. Sobel and Dr. E. T. Coffey for sharing reagents and Kelli Simburger and Sylvia Johnson for technical support. We used the Bakewell Neuroimaging facility for live imaging. This work was sup-

ported by National Institutes of Health (NIH) Grants NS065053 (to A.D. and J.M.), AG013730 (to J.M.), and NS060709 (to V.C.), by P30 NIH Neuroscience Blueprint Core Grant NS057105 to Washington University, and by the Edward Mallinckrodt, Jr. Foundation (V.C.).

1. Coleman MP, Perry VH (2002) Axon pathology in neurological disease: A neglected therapeutic target. *Trends Neurosci* 25(10):532–537.
2. Luo L, O'Leary DD (2005) Axon retraction and degeneration in development and disease. *Annu Rev Neurosci* 28:127–156.
3. Rosenthal S, Kaufman S (1974) Vincristine neurotoxicity. *Ann Intern Med* 80(6):733–737.
4. Höke A (2006) Neuroprotection in the peripheral nervous system: Rationale for more effective therapies. *Arch Neurol* 63(12):1681–1685.
5. Araki T, Sasaki Y, Milbrandt J (2004) Increased nuclear NAD biosynthesis and SIRT1 activation prevent axonal degeneration. *Science* 305(5686):1010–1013.
6. Avery MA, Sheehan AE, Kerr KS, Wang J, Freeman MR (2009) Wld S requires Nmnat1 enzymatic activity and N16-VCP interactions to suppress Wallerian degeneration. *J Cell Biol* 184(4):501–513.
7. Conforti L, et al. (2000) A Ufd2/D4Cole1e chimeric protein and overexpression of Rbp7 in the slow Wallerian degeneration (WldS) mouse. *Proc Natl Acad Sci USA* 97(21): 11377–11382.
8. Conforti L, et al. (2009) Wld S protein requires Nmnat activity and a short N-terminal sequence to protect axons in mice. *J Cell Biol* 184(4):491–500.
9. Mack TG, et al. (2001) Wallerian degeneration of injured axons and synapses is delayed by a Ube4b/Nmnat chimeric gene. *Nat Neurosci* 4(12):1199–1206.
10. Wang JT, Medress ZA, Barres BA (2012) Axon degeneration: Molecular mechanisms of a self-destruction pathway. *J Cell Biol* 196(1):7–18.
11. Zhai Q, et al. (2003) Involvement of the ubiquitin-proteasome system in the early stages of wallerian degeneration. *Neuron* 39(2):217–225.
12. Gilley J, Coleman MP (2010) Endogenous Nmnat2 is an essential survival factor for maintenance of healthy axons. *PLoS Biol* 8(1):e1000300.
13. Barnat M, et al. (2010) Distinct roles of c-Jun N-terminal kinase isoforms in neurite initiation and elongation during axonal regeneration. *J Neurosci* 30(23):7804–7816.
14. Kenney AM, Kocsis JD (1998) Peripheral axotomy induces long-term c-Jun amino-terminal kinase-1 activation and activator protein-1 binding activity by c-Jun and junD in adult rat dorsal root ganglia In vivo. *J Neurosci* 18(4):1318–1328.
15. Lindwall C, Dahlin L, Lundborg G, Kanje M (2004) Inhibition of c-Jun phosphorylation reduces axonal outgrowth of adult rat nodose ganglia and dorsal root ganglia sensory neurons. *Mol Cell Neurosci* 27(3):267–279.
16. Miller BR, et al. (2009) A dual leucine kinase-dependent axon self-destruction program promotes Wallerian degeneration. *Nat Neurosci* 12(4):387–389.
17. Nix P, Hisamoto N, Matsumoto K, Bastiani M (2011) Axon regeneration requires coordinate activation of p38 and JNK MAPK pathways. *Proc Natl Acad Sci USA* 108 (26):10738–10743.
18. Xia Z, Dickens M, Raingeaud J, Davis RJ, Greenberg ME (1995) Opposing effects of ERK and JNK-p38 MAP kinases on apoptosis. *Science* 270(5240):1326–1331.
19. Xiong X, Collins CA (2012) A conditioning lesion protects axons from degeneration via the Wallenda/DLK MAP kinase signaling cascade. *J Neurosci* 32(2):610–615.
20. Xiong X, et al. (2010) Protein turnover of the Wallenda/DLK kinase regulates a retrograde response to axonal injury. *J Cell Biol* 191(1):211–223.
21. Yoshimura K, et al. (2011) c-Jun N-terminal kinase induces axonal degeneration and limits motor recovery after spinal cord injury in mice. *Neurosci Res* 71(3):266–277.
22. Tararuk T, et al. (2006) JNK1 phosphorylation of SCG10 determines microtubule dynamics and axodendritic length. *J Cell Biol* 173(2):265–277.
23. Riederer BM, et al. (1997) Regulation of microtubule dynamics by the neuronal growth-associated protein SCG10. *Proc Natl Acad Sci USA* 94(2):741–745.
24. Antonsson B, et al. (1998) Identification of in vitro phosphorylation sites in the growth cone protein SCG10. Effect Of phosphorylation site mutants on microtubule-destabilizing activity. *J Biol Chem* 273(14):8439–8446.
25. Sasaki Y, Araki T, Milbrandt J (2006) Stimulation of nicotinamide adenine dinucleotide biosynthetic pathways delays axonal degeneration after axotomy. *J Neurosci* 26(33): 8484–8491.
26. Beirowski B, et al. (2005) The progressive nature of Wallerian degeneration in wild-type and slow Wallerian degeneration (WldS) nerves. *BMC Neurosci* 6:6.
27. Chao DT, et al. (1995) Bcl-XL and Bcl-2 repress a common pathway of cell death. *J Exp Med* 182(3):821–828.
28. Gerdts J, Sasaki Y, Vohra B, Marasa J, Milbrandt J (2011) Image-based screening identifies novel roles for IkappaB kinase and glycogen synthase kinase 3 in axonal degeneration. *J Biol Chem* 286(32):28011–28018.
29. Vohra BP, et al. (2010) Amyloid precursor protein cleavage-dependent and -independent axonal degeneration programs share a common nicotinamide mononucleotide adenylyltransferase 1-sensitive pathway. *J Neurosci* 30(41):13729–13738.
30. Sasaki Y, Vohra BP, Lund FE, Milbrandt J (2009) Nicotinamide mononucleotide adenylyl transferase-mediated axonal protection requires enzymatic activity but not increased levels of neuronal nicotinamide adenine dinucleotide. *J Neurosci* 29(17): 5525–5535.
31. Coleman MP, Freeman MR (2010) Wallerian degeneration, wld(s), and nmnat. *Annu Rev Neurosci* 33:245–267.
32. Court FA, Coleman MP (2012) Mitochondria as a central sensor for axonal degenerative stimuli. *Trends Neurosci* 35(6):364–372.
33. De Vos KJ, Grierson AJ, Ackerley S, Miller CC (2008) Role of axonal transport in neurodegenerative diseases. *Annu Rev Neurosci* 31:151–173.
34. Avery MA, et al. (2012) WldS prevents axon degeneration through increased mitochondrial flux and enhanced mitochondrial Ca2+ buffering. *Curr Biol* 22(7): 596–600.
35. Barrientos SA, et al. (2011) Axonal degeneration is mediated by the mitochondrial permeability transition pore. *J Neurosci* 31(3):966–978.
36. Hunter T (2007) The age of crosstalk: Phosphorylation, ubiquitination, and beyond. *Mol Cell* 28(5):730–738.
37. Vega IE, Hamano T, Propost JA, Grenningloh G, Yen SH (2006) Taxol and tau overexpression induced calpain-dependent degradation of the microtubule-destabilizing protein SCG10. *Exp Neurol* 202(1):152–160.
38. Camoletto P, Colesanti A, Ozon S, Sobel A, Fasolo A (2001) Expression of stathmin and SCG10 proteins in the olfactory neurogenesis during development and after lesion in the adulthood. *Brain Res Bull* 54(1):19–28.
39. Pellier-Monnin V, Astic L, Bichet S, Riederer BM, Grenningloh G (2001) Expression of SCG10 and stathmin proteins in the rat olfactory system during development and axonal regeneration. *J Comp Neurol* 433(2):239–254.
40. Voria I, et al. (2006) Improved sciatic nerve regeneration by local thyroid hormone treatment in adult rat is accompanied by increased expression of SCG10. *Exp Neurol* 197(1):258–267.
41. Li YH, et al. (2009) Rnd1 regulates axon extension by enhancing the microtubule destabilizing activity of SCG10. *J Biol Chem* 284(1):363–371.
42. Morii H, Shiraishi-Yamaguchi Y, Mori N (2006) SCG10, a microtubule destabilizing factor, stimulates the neurite outgrowth by modulating microtubule dynamics in rat hippocampal primary cultured neurons. *J Neurobiol* 66(10):1101–1114.
43. Xu H, Dhanasekaran DN, Lee CM, Reddy EP (2010) Regulation of neurite outgrowth by interactions between the scaffolding protein, JNK-associated leucine zipper protein, and neuronal growth-associated protein superior cervical ganglia clone 10. *J Biol Chem* 285(6):3548–3553.
44. Carmichael ST, et al. (2005) Growth-associated gene expression after stroke: Evidence for a growth-promoting region in peri-infarct cortex. *Exp Neurol* 193(2):291–311.
45. Mason MR, Lieberman AR, Grenningloh G, Anderson PN (2002) Transcriptional upregulation of SCG10 and CAP-23 is correlated with regeneration of the axons of peripheral and central neurons in vivo. *Mol Cell Neurosci* 20(4):595–615.
46. Shin JE, et al. (2012) Dual leucine zipper kinase is required for retrograde injury signaling and axonal regeneration. *Neuron* 74(6):1015–1022.
47. Lipton RB, et al. (1989) Taxol produces a predominantly sensory neuropathy. *Neurology* 39(3):368–373.
48. Cortes J, Baselga J (2007) Targeting the microtubules in breast cancer beyond taxanes: The epothilones. *Oncologist* 12(3):271–280.
49. Graf ER, Heerssen HM, Wright CM, Davis GW, DiAntonio A (2011) Stathmin is required for stability of the Drosophila neuromuscular junction. *J Neurosci* 31(42): 15026–15034.
50. Ozon S, Maucuer A, Sobel A (1997) The stathmin family — molecular and biological characterization of novel mammalian proteins expressed in the nervous system. *Eur J Biochem* 248(3):794–806.